Use of Piezoelectric Shear Response in Adaptive Sandwich Shells of Revolution - Part 1: Theoretical Formulation

Ayech Benjeddou, V. Gorge, Roger Ohayon

▶ **To cite this version:**

Ayech Benjeddou, V. Gorge, Roger Ohayon. Use of Piezoelectric Shear Response in Adaptive Sandwich Shells of Revolution - Part 1: Theoretical Formulation. Journal of Intelligent Material Systems and Structures, 2001, 12 (4), pp.235-245. 10.1106/m11m-v7nl-00re-ha3j . hal-03179646

HAL Id: hal-03179646
https://hal.science/hal-03179646v1

Submitted on 1 Sep 2023

HAL is a multi-disciplinary open access archive for the deposit and dissemination of scientific research documents, whether they are published or not. The documents may come from teaching and research institutions in France or abroad, or from public or private research centers.

L'archive ouverte pluridisciplinaire **HAL**, est destinée au dépôt et à la diffusion de documents scientifiques de niveau recherche, publiés ou non, émanant des établissements d'enseignement et de recherche français ou étrangers, des laboratoires publics ou privés.

Use of Piezoelectric Shear Response in Adaptive Sandwich Shells of Revolution – Part 1: Theoretical Formulation

A. BENJEDDOU, V. GORGE AND R. OHAYON*

Structural Mechanics and Coupled Systems Laboratory, Conservatoire National des Arts et Métiers, 2 rue Conté, 75003 Paris, France.

ABSTRACT: This work, in two parts, proposes a theoretical formulation (Part 1) and its finite element implementation (Part 2) for an adaptive sandwich shell of revolution that uses the transverse shear response of a piezoelectric core sandwiched between two elastic faces. For this, the former is assumed initially poled along the meridian but subjected to electric potentials on its fully electroded inner and outer surfaces. The model assumes the first-order shear deformation theory for each layer and enforces the displacement continuity conditions at the core to faces interfaces. Besides, the sandwich theory retains the shell transverse deflection together with the mean and relative tangential displacements and bending rotations of the elastic faces as mechanical independent variables. These are augmented by the electric potential in the piezoelectric core, in order to effectively consider the electromechanical coupling. Implementation and validation of the theoretical formulation developed in this part are presented in Part 2 of the paper.

INTRODUCTION

APPLICATION of a voltage difference on covering electrodes perpendicular to the initial poling direction of an embedded piezoelectric material induces transverse shear strains that bend the host structure. Conversely, bending of the latter induces a difference of potentials on the same electrodes due to the transverse shear deformation of the embedded piezoelectric material. This defines the so-called piezoelectric *shear actuation/sensing mechanism*, in opposition to the conventional extension actuation/sensing one obtained for an applied electric field parallel to the initial polarization, both generally through-thickness.

The shear response of the piezoceramics was used in ultrasonic transducers applications since the early sixties (Bradley and Bergman, 1963). It was theoretically studied since the mid-seventies for the axisymmetric behavior of hollow cylinders (Adelman and Stavsky, 1975). Extension was then made to single-layer shells of revolution at the end of that decade (Boriseiko et al., 1979) and to arbitrary shells (Rogacheva, 1981; Parton and Senik, 1984) at the early eighties. Several electro-acoustic devices have then been developed using the shear response of piezoceramics such as, torsional vibrators (Aoyagi et al., 1977), piezoelectric motors (Glazounov et al., 1999, 2000), and torsional actuators (Glazounov et al., 1998, 2000; Centalanza and Smith, 2000).

Although well known by the acoustics and materials communities, the shear response of piezoceramics was used in smart structure applications only by the mid-nineties. Hence, Sun and Zhang (1995) have presented a preliminary static evaluation for adaptive sandwich beams using a commercial finite element analysis code, followed by a theoretical static formulation and analysis (Zhang and Sun, 1996), recently extended to adaptive sandwich plates (Zhang and Sun, 1999). Two models were then proposed by Benjeddou et al. (1997, 1999a) using either the core (Benjeddou et al., 1997) or faces (Benjeddo et al., 1999a) mean and relative displacements as independent variables. Comparison of both extension and shear actuation mechanisms (Benjeddou et al., 2000) using both models (Benjeddou et al., 1999b) has shown that the model using faces displacements has better convergence characteristics. The corresponding model (Benjeddou et al., 1999a) has then been retained for active vibration control of sandwich beams (Trindade et al., 1999). Analytical models and exact solution for beams with extension and shear actuators have been also presented recently (Aldraihem and Khdeir, 2000) using first and higher-order beam theories and state space solution technique. It was found that unlike extension actuator, the shear one can generate deflection of clamped-clamped beams.

Recent literature review (Saravanos and Heyliger, 1999) and survey (Benjeddou, 2000a) indicate that the piezoelectric shear actuation mechanism was not

*Author to whom correspondence should be addressed.
E-mail: ohayon@cnam.fr

investigated for smart shells. However, theoretical formulations and analyses have been recently presented for both arbitrary (Benjeddou, 2000b) and axisymmetric (Benjeddou, 2000c) adaptive sandwich shells. In both formulations the electric potential in the in-plane polarized and fully electroded piezoelectric core sandwiched between elastic faces has been considered uniform and through-thickness linear. Corresponding numerical formulations and analyses are thus still to be made. Therefore, it is the aim of this work to present, in two parts, the theoretical (Part 1) and finite element (Part 2) formulations of an adaptive sandwich shell of revolution that uses the transverse shear mode of piezoelectric materials.

In the following, a first-order shear deformation theory is presented for axisymmetric adaptive sandwich shells. It is based on displacement continuities at the piezoelectric core inner and outer interfaces. The mean and relative face displacements, introduced in (Benjeddou and Hamdi, 1996), are augmented by the mean and relative face rotations and used as independent mechanical variables. The piezoelectric core is assumed polarized along the shell meridian and fully electroded on its inner and outer surfaces. The electric potential inside the piezoelectric core is assumed linear through its thickness and retained as an independent electric variable in order to consider effectively the piezoelectric coupling. An extended d'Alembert or virtual works principle is used to derive the variational formulation of the piezoelectric adaptive sandwich shell of revolution.

MODEL ASSUMPTIONS

Lets consider the adaptive sandwich shell of revolution, represented by its meridian section in Figure 1. It is composed of a piezoelectric core sandwiched between elastic faces. Its theoretical formulation is based on the following assumptions:

1. Mechanical and electric quantities are sufficiently small so that linear theories of elasticity and piezoelectricity apply.
2. Elastic and piezoelectric materials are considered orthotropic with axes of material symmetry coinciding with the sandwich shell main curvatures.
3. The total thickness of the adaptive sandwich shell is very small compared with the smallest radius of curvature.
4. The normal stresses in the thickness direction are considered small compared with the other stresses and can be neglected.
5. The transverse displacement of all layers is assumed through-thickness constant.
6. All layers of the sandwich shell are supposed perfectly bonded.

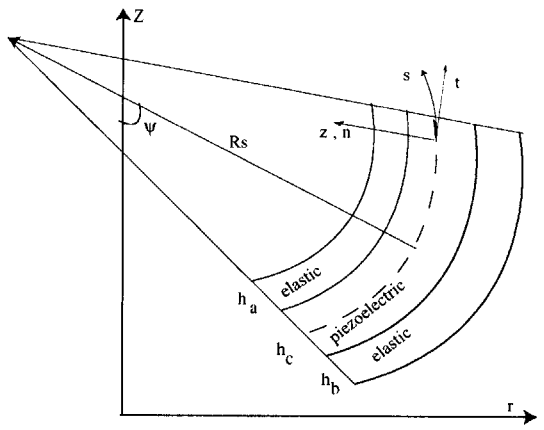

Figure 1. *The sandwich shell of revolution configuration: geometry and notations*

7. All layers can resist membrane, bending and transverse shear stresses.
8. Translation, rotary and their coupling inertia effects are taken into account.
9. The piezoelectric core is supposed polarized along its meridian, fully electroded on its inner and outer surfaces but unelectroded on its edges.
10. The electric potential inside the piezoelectric core is assumed through-thickness linear.

SANDWICH SHELL DISPLACEMENTS AND STRAINS

According to above 5th and 7th assumptions, the mechanical displacements in each layer are considered through thickness linear; that is, for the kth layer

$$\begin{aligned} \underline{u}^k(s,\theta,z) &= u^k(s,\theta) + (z - z_k)\beta^k(s,\theta) \\ \underline{v}^k(s,\theta,z) &= v^k(s,\theta) + (z - z_k)\beta^k_\theta(s,\theta) \\ \underline{w}^k(s,\theta,z) &= w(s,\theta) \end{aligned} \tag{1}$$

where $z_a = (h_a + h_c)/2$, $z_c = 0$, $z_b = -(h_b + h_c)/2$. u^k, v^k, w, β^k, β^k_θ, are the displacements in the s, θ, z directions of the kth layer middle surface and the rotations of its normal in the s–z, and θ–z planes, respectively.

Following the 6th basic assumption, above displacements are made continuous at the core interfaces with faces. They are then written in terms of the following mean and relative faces tangential displacements, introduced in (Benjeddou and Hamdi, 1996), and their mean and relative bending rotations, denoted as

$$\bar{x} = (x^a + x^b)/2; \quad \tilde{x} = (x^a - x^b) \tag{2}$$

where $x = u,\ v,\ \beta,\ \beta_\theta$ representing either of the tangential displacements and bending rotations in the planes s–z and θ–z, respectively. With these notations, the displacements in the fth face can then be written as

$$\begin{aligned}\underline{u}^f &= (\bar{u} \pm \tilde{u}/2) + (z - z_f)(\bar{\beta} \pm \tilde{\beta}/2)\\ \underline{v}^f &= (\bar{v} \pm \tilde{v}/2) + (z - z_f)(\bar{\beta}_\theta \pm \tilde{\beta}_\theta/2)\\ \underline{w}^f &= w\end{aligned} \tag{3}$$

where the '+' sign is for the inner face ($f = a$) and the '−' for the outer one ($f = b$).

With notations (2) in mind, the core displacements can be written in the form

$$\begin{aligned}\underline{u}^c &= \bar{u} - \frac{\tilde{h}}{4}\bar{\beta} - \frac{\bar{h}}{4}\tilde{\beta}\Big) + z\left(\frac{\tilde{u}}{h_c} - \frac{\bar{h}}{h_c}\bar{\beta} - \frac{\tilde{h}}{4h_c}\tilde{\beta}\right)\\ \underline{v}^c &= \bar{v} - \frac{\tilde{h}}{4}\bar{\beta}_\theta - \frac{\bar{h}}{4}\tilde{\beta}_\theta\Big) + z\ \frac{\tilde{v}}{h_c} - \frac{\bar{h}}{h_c}\bar{\beta}_\theta - \frac{\tilde{h}}{4h_c}\tilde{\beta}_\theta\Big)\\ \underline{w}^c &= w\end{aligned} \tag{4}$$

where $\bar{h}, \tilde{h}$ are the mean and relative faces thicknesses defined as in (2). Notice the appearance of two shear rotations $\tilde{u}/h_c$ and $\tilde{v}/h_c$, resulting from the sliding of the faces against the core. They are characteristic of any sandwich theory that retains the faces displacements as independent variables. Nevertheless, such sandwich formulation does not allow for zero-thickness core. If this is required, the core displacements and rotations should be retained as independent variables, together with the face rotations. However, the sliding rotations will no longer appear explicitly in the core displacements as in (4).

Applying the usual strain-displacement relations to Equations (3), leads to the following fth face in-plane and transverse shear strains, respectively

$$\begin{aligned}\{\varepsilon^f\} &= (\{\bar{e}\} \pm \{\tilde{e}\}/2) + (z - z_f)(\{\bar{\chi}\} \pm \{\tilde{\chi}\}/2)\\ \{\gamma^f\} &= (\{\bar{\gamma}\} \pm \{\tilde{\gamma}\}/2)\end{aligned} \tag{5}$$

where the mean and relative membrane $\{\bar{e}\}$, $\{\tilde{e}\}$, bending, $\{\bar{\chi}\}$, $\{\tilde{\chi}\}$ and shear $\{\bar{\gamma}\}$, $\{\tilde{\gamma}\}$ strain vectors are given in Benjeddou (2000c).

Similarly, using Equations (4) in the usual strain-displacement relations, leads to the following core in-plane and transverse shear strains

$$\begin{aligned}\{\varepsilon^c\} &= \{\bar{e}\} - \frac{\tilde{h}}{4}\{\bar{\chi}\} - \frac{\bar{h}}{4}\{\tilde{\chi}\}\Big) + z\left(\frac{1}{h_c}\{\tilde{e}\} - \frac{\bar{h}}{h_c}\{\bar{\chi}\} - \frac{\tilde{h}}{4h_c}\{\tilde{\chi}\}\right)\\ \{\gamma^c\} &= (\{\bar{\gamma}^c\} + \{\tilde{\gamma}^c\})\end{aligned} \tag{6}$$

Mean, $\{\bar{\gamma}^c\}$, and relative, $\{\tilde{\gamma}^c\}$, transverse shear strains can also be found in Benjeddou (2000c). As for the core displacement (4), notice the appearance of the sliding curvatures $\{\tilde{e}\}/h_c$, in the core bending strains. The shear strain decomposition in $(6)_2$ is different from that in $(5)_2$ due to the presence of the sliding rotations in the former expressions. Hence, the relative displacements of the faces can both bend and shear the shell. This explicit representation of the transverse shear due to the sandwich construction is a nice feature for the piezoelectric shear actuation mechanism as will be shown later. This motivated the decomposition into mean and relative quantities in the whole formulation.

PIEZOELECTRIC CORE ELECTRIC POTENTIAL AND FIELD

Following the last assumption, the electric potential in the piezoelectric core has the form

$$\varphi(s, \theta, z) = \bar{\varphi}(s, \theta) + z\tilde{\varphi}(s, \theta)/h_c \tag{7}$$

where $\bar{\varphi}$, $\tilde{\varphi}$ follow notations (2) for the prescribed or generated potentials φ^+ and φ^- on the inner and outer skins of the core layer, respectively.

Introducing Equation (7) in the usual electric field-potential relation leads to the following expressions for the in-plane, (p), and transverse, (z), electric field components

$$\begin{aligned}\{E_p(s, \theta, z)\} &= \{\bar{E}(s, \theta)\} + z\{\tilde{E}(s, \theta)\}\\ E_z(s, \theta, z) &= -\tilde{\varphi}(s, \theta)/h_c\end{aligned} \tag{8}$$

with

$$\langle E_p \rangle = \langle\, E_s \quad E_\theta \,\rangle, \quad \langle \bar{E} \rangle = \langle\, \bar{E}_s \quad \bar{E}_\theta \,\rangle, \quad \langle \tilde{E} \rangle = \langle\, \tilde{E}_s \quad \tilde{E}_\theta \,\rangle$$

$$\bar{E}_s = -\bar{\varphi}_{,s}, \quad \bar{E}_\theta = -\frac{1}{r}\bar{\varphi}_{,\theta} \quad \tilde{E}_s = -\tilde{\varphi}_{,s}/h_c, \quad \tilde{E}_\theta = -\frac{1}{r}\tilde{\varphi}_{,\theta}/h_c$$

Notice that for uniform potentials, $\bar{\varphi}$ and $\tilde{\varphi}$, the in-plane electric field components vanish, and only Equation $(8)_2$ holds.

ZERO NORMAL STRESS REDUCED CONSTITUTIVE EQUATIONS

According to the 4th assumption, the normal stress is neglected. Hence, the normal strain is no longer nil as might be understood from the displacement (1), but computed from this assumption. The resulting relation is then back substituted into the in-plane converse piezoelectric constitutive equations. Hence, the following reduced in-plane and transverse converse piezoelectric constitutive equations for the core are obtained

$$\begin{aligned}\{\sigma^c\} &= [Q^c]\{\varepsilon^c\} - [e_p]^T\{E_p\}\\ \{\tau^c\} &= [Q_s^c]\{\gamma^c\} - \{e_s\}E_z\end{aligned} \tag{9}$$

where in-plane and transverse elastic and piezoelectric matrices are given in Appendix A.

Similarly, the back substitution of the normal strain expression, deduced from the zero–normal stress condition, leads to the following reduced in-plane and transverse reduced direct piezoelectric constitutive equations, respectively

$$\begin{aligned} \{D_p\} &= [e_p]\{\varepsilon^c\} + [\in_p]\{E_p\} \\ D_z &= \langle e_s\rangle\{\gamma^c\} + \in_{zz} E_z \end{aligned} \tag{10}$$

In-plane and transverse piezoelectric and dielectric matrices are given also in Appendix A.

From Equations (9) and (10), it is worthy to notice that the in-plane and transverse electromechanical behaviors are uncoupled. Moreover, for uniform potentials, the in-plane electric field components vanish (see Equation (8)). Hence, the electromechanical coupling becomes present only for the transverse behavior. That is, between the transverse shear strains and transverse electric field component. This defines the so-called *shear actuation/ sensing mechanism* (Benjeddou et al., 2000).

The zero normal stress reduced in-plane and transverse elastic constitutive equations of the faces are deduced from the previous converse ones (9) by substituting the superscript c with $f=a$, b and vanishing the piezoelectric constants

$$\begin{aligned} \{\sigma^f\} &= [Q^f]\{\varepsilon^f\} \\ \{\tau^f\} &= [Q_s^f]\{\gamma^f\} \end{aligned} \tag{11}$$

The in-plane, $[Q^f]$, and shear, $\left[Q_s^f\right]$, elastic matrices of the faces have the same form as those of the piezoelectric core, given in Appendix A.

VARIATIONAL FORMULATION

For admissible virtual displacements, $\delta\bar{u}$, $\delta\bar{v}$, δw, $\delta\bar{\beta}$, $\delta\bar{\beta}_\theta$, $\delta\tilde{u}$, $\delta\tilde{v}$, $\delta\tilde{\beta}$, $\delta\tilde{\beta}_\theta$ and electric potentials, $\delta\bar{\varphi}$, $\delta\tilde{\varphi}$, the extended d'Alembert principle applied to the adaptive shell, is

$$\delta W_{\text{int}} - \delta W_{\text{in}} - \delta W_{\text{ext}} = 0 \tag{12}$$

where $\delta\mathrm{W}_{\text{int}}$, $\delta\mathrm{W}_{\text{in}}$, $\delta\mathrm{W}_{\text{ext}}$ are the sandwich shell internal, inertia and external virtual works.

Sandwich Shell Internal Virtual Work

The adaptive sandwich shell internal virtual work can be written as

$$\begin{aligned} \delta W_{\text{int}} = &\sum_{k=a}^{c}\int_{\Omega^k}\left(\langle\delta\varepsilon^k\rangle\left\{\sigma^k\right\} + \langle\delta\gamma^k\rangle\left\{\tau^k\right\}\right)d\Omega^k \\ &- \int_{\Omega^c}\left(\langle\delta E_p\rangle\left\{D_p\right\} + \delta E_z D_z\right)d\Omega^c \end{aligned} \tag{13}$$

where Ω^{k} is the domain volume of the kth layer.

Substituting the constitutive equations (9–11) in the previous relation and decomposing it into mechanical, (m), piezoelectric, (p), and electric, (e), contributions leads to

$$\delta W_{\text{int}} = \delta W_{\text{int}}^m - \delta W_{\text{int}}^p - \delta W_{\text{int}}^e \tag{14}$$

with

$$\begin{aligned} \delta W_{\text{int}}^m &= \sum_{k=a}^{c}\int_{\Omega^k}\left(\langle\delta\varepsilon^k\rangle[Q^k]\left\{\varepsilon^k\right\} + \langle\delta\gamma^k\rangle[Q_s^k]\left\{\gamma^k\right\}\right)d\Omega^k \\ \delta W_{\text{int}}^e &= \int_{\Omega^c}\left(\langle\delta E_p\rangle[\in_p]\left\{E_p\right\} + \delta E_z \in_{zz} E_z\right)d\Omega^c \\ \delta W_{\text{int}}^p &= \int_{\Omega^c}\left(\langle\delta\varepsilon^c\rangle[e_p]^T\left\{E_p\right\} + \langle\delta\gamma^c\rangle\{e_s\}E_z\right)d\Omega^c \\ &\quad + \int_{\Omega^c}\left(\langle\delta E_p\rangle[e_p]\{\varepsilon^c\} + \delta E_z\langle e_s\rangle\left\{\gamma^c\right\}\right)d\Omega^c \end{aligned}$$

These expressions are now further decomposed into mean and relative contributions using the strain and field relations (5–8) and explicit integration through the shell thickness.

MECHANICAL INTERNAL VIRTUAL WORK

Substituting the strain Equations (5, 6) in the mechanical internal virtual work, defined in Equation (14), and integrating explicitly through the shell thickness, then separating the resulting relation into extension, (e), bending, (χ), and shear, (γ), contributions lead to

$$\delta W_{\text{int}}^m = \delta W_e^m + \delta W_{e\chi}^m + \delta W_\chi^m + \delta W_\gamma^m \tag{15}$$

δW_e^m is the extension (or membrane) internal virtual work of the sandwich shell given by

$$\begin{aligned} \delta W_e^m = &\int_A\left(\langle\delta\bar{e}\rangle[\bar{D}_e]\{\bar{e}\} + \langle\delta\bar{e}\rangle[\bar{\tilde{D}}_e]\{\tilde{e}\}\right)dA \\ &+ \int_A\left(\langle\delta\tilde{e}\rangle[\bar{\tilde{D}}_e]\{\bar{e}\} + \langle\delta\tilde{e}\rangle[\tilde{D}_e]\{\tilde{e}\}\right)dA \end{aligned} \tag{16}$$

where A is the area of the shell middle surface and the membrane elastic matrices are detailed in Appendix B. They indicate that the mean-relative membrane coupling, present in Equation (16), vanishes for symmetric sandwich shells.

The extension-bending internal virtual work of the sandwich shell is given by

$$\begin{aligned} \delta W_{e\chi}^m = &\int_A\left(\langle\delta\bar{e}\rangle[\bar{D}_{e\chi}]\{\bar{\chi}\} + \langle\delta\bar{\chi}\rangle[\bar{D}_{e\chi}]\{\bar{e}\}\right)dA \\ &+ \int_A\left(\langle\delta\bar{e}\rangle[\bar{\tilde{D}}_{e\chi}]\{\tilde{\chi}\} + \langle\delta\tilde{\chi}\rangle[\bar{\tilde{D}}_{e\chi}]\{\bar{e}\}\right)dA \\ &+ \int_A\left(\langle\delta\tilde{e}\rangle[\bar{\tilde{D}}_{\chi e}]\{\bar{\chi}\} + \langle\delta\bar{\chi}\rangle[\bar{\tilde{D}}_{\chi e}]\{\tilde{e}\}\right)dA \\ &+ \int_A\left(\langle\delta\tilde{e}\rangle[\bar{\tilde{D}}_{e\chi}]\{\tilde{\chi}\} + \langle\delta\tilde{\chi}\rangle[\tilde{D}_{e\chi}]\{\tilde{e}\}\right)dA \end{aligned} \tag{17}$$

All elastic membrane-bending matrices are detailed in Appendix B. They show that there are four types of mechanical couplings that are localized in the core:

- A geometrical coupling between the *mean membrane* and *bending* strains which vanishes for geometrical symmetry (i.e. identical face thicknesses).
- A coupling between the *mean membrane* and *relative bending* strains.
- A coupling between the *relative membrane* and *mean bending* strains.
- A geometrical coupling between the *relative membrane* and *bending* strains, which vanishes for identical faces thicknesses.

The bending internal virtual work of the sandwich shell can be written as

$$\delta W_\chi^m = \int_A \left(\langle \delta\bar{\chi} \rangle [\bar{D}_\chi] \{\bar{\chi}\} + \langle \delta\bar{\chi} \rangle \left[\tilde{\bar{D}}_\chi\right] \{\tilde{\chi}\} \right) dA + \int_A \left(\langle \delta\tilde{\chi} \rangle \left[\tilde{\bar{D}}_\chi\right] \{\bar{\chi}\} + \langle \delta\tilde{\chi} \rangle [\tilde{D}_\chi] \{\tilde{\chi}\} \right) dA \quad (18)$$

The bending elastic matrices, given in Appendix B, indicate that the mean-relative bending coupling, in Equation (18), vanishes for symmetric sandwich constructions.

The shear internal virtual work, in Equation (15), is defined by

$$\begin{aligned} \delta W_\gamma^m = & \int_A \left(\langle \delta\bar{\gamma} \rangle \left[\bar{D}_\gamma\right] \{\bar{\gamma}\} + \langle \delta\bar{\gamma} \rangle \left[\tilde{\bar{D}}_\gamma\right] \{\tilde{\gamma}\} \right) dA \\ & + \int_A \left(\langle \delta\tilde{\gamma} \rangle \left[\tilde{\bar{D}}_\gamma\right] \{\bar{\gamma}\} + \langle \delta\tilde{\gamma} \rangle \left[\tilde{D}_\gamma\right] \{\tilde{\gamma}\} \right) dA \\ & + \int_A \left(\langle \delta\bar{\gamma}^c \rangle \left[\bar{D}_\gamma^c\right] \{\bar{\gamma}^c\} + \langle \delta\bar{\gamma}^c \rangle \left[\tilde{\bar{D}}_\gamma^c\right] \{\tilde{\gamma}^c\} \right) dA \\ & + \int_A \left(\langle \delta\tilde{\gamma}^c \rangle \left[\tilde{\bar{D}}_\gamma^c\right] \{\bar{\gamma}^c\} + \langle \delta\tilde{\gamma}^c \rangle \left[\tilde{D}_\gamma^c\right] \{\tilde{\gamma}^c\} \right) dA \end{aligned} \quad (19)$$

Shear elastic matrices, given in Appendix B, show that the mean-relative shear coupling present in the faces vanishes for symmetric sandwich shells.

PIEZOELECTRIC INTERNAL VIRTUAL WORK

Substituting the core strains (6) in the piezoelectric internal virtual work, defined in Equation (14), and integrating analytically through the shell thickness, then separating into extension, bending and shear contributions, lead to

$$\delta W_{\text{int}}^p = \delta W_e^p + \delta W_\chi^p + \delta W_\gamma^p \quad (20)$$

δW_e^p is the extension-piezoelectric internal virtual work defined as

$$\delta W_e^p = \int_A \left(\langle \delta\bar{e} \rangle \left[\bar{D}_e^p\right]^T \{\bar{E}\} + \langle \delta\bar{E} \rangle \left[\bar{D}_e^p\right] \{\bar{e}\} \right) dA + \int_A \left(\langle \delta\tilde{e} \rangle \left[\tilde{D}_e^p\right]^T \{\tilde{E}\} + \langle \delta\tilde{E} \rangle \left[\tilde{D}_e^p\right] \{\tilde{e}\} \right) dA \quad (21)$$

where the extension piezoelectric matrices are given in Appendix B. It is clear from Equation (21) that this electromechanical coupling is either between the mean or relative membrane strains and in-plane electric field components. This means that this work vanishes for uniform electric potentials since the latter is nil in this case.

δW_χ^p is the bending piezoelectric internal virtual work. It can be written in the form

$$\begin{aligned} \delta W_\chi^p = & \int_A \left(\langle \delta\bar{\chi} \rangle \left[\bar{D}_\chi^p\right] \{\bar{E}\} + \langle \delta\bar{E} \rangle \left[\bar{D}_\chi^p\right]^T \{\bar{\chi}\} \right) dA \\ & + \int_A \left(\langle \delta\bar{\chi} \rangle \left[\tilde{\bar{D}}_\chi^p\right] \{\tilde{E}\} + \langle \delta\tilde{E} \rangle \left[\tilde{\bar{D}}_\chi^p\right]^T \{\bar{\chi}\} \right) dA \\ & + \int_A \left(\langle \delta\tilde{\chi} \rangle \left[\tilde{\bar{D}}_\chi^p\right] \{\bar{E}\} + \langle \delta\bar{E} \rangle \left[\tilde{\bar{D}}_\chi^p\right]^T \{\tilde{\chi}\} \right) dA \\ & + \int_A \left(\langle \delta\tilde{\chi} \rangle \left[\tilde{D}_\chi^p\right] \{\tilde{E}\} + \langle \delta\tilde{E} \rangle \left[\tilde{D}_\chi^p\right]^T \{\tilde{\chi}\} \right) dA \end{aligned} \quad (22)$$

The bending piezoelectric matrices, given in Appendix B, and Equation (22) indicate that there are four types of electromechanical couplings

- A geometrical coupling between the *mean bending strains* and *in-plane electric fields*, that vanishes for identical thickness faces.
- A coupling between *mean bending strains* and *relative in-plane electric fields*.
- A coupling between *relative bending strains* and *mean in-plane electric fields*.
- A geometrical coupling between the *relative bending strains* and *in-plane electric fields* that also vanishes for identical thickness faces.

It is then clear that, for symmetric sandwich constructions, a mean in-plane electric field can produce relative bending strains only and *vice versa*. Also, a relative in-plane electric field can produce mean bending strains only and *vice versa*. As for the extension piezoelectric work (21), the bending one (22) also vanishes for uniform potentials.

The shear piezoelectric internal virtual work δW_γ^p, in Equation (20), can be written as

$$\delta W_\gamma^p = \int_A \left(\langle \delta\bar{\gamma}^c \rangle \left\{\bar{D}_\gamma^p\right\} E_z + \delta E_z \langle \bar{D}_\gamma^p \rangle \{\bar{\gamma}^c\} \right) dA + \int_A \left(\langle \delta\tilde{\gamma}^c \rangle \left\{\tilde{D}_\gamma^p\right\} E_z + \delta E_z \langle \tilde{D}_\gamma^p \rangle \{\tilde{\gamma}^c\} \right) dA \quad (23)$$

where the vectors of the shear piezoelectric coupling constants are given in Appendix B. Here, the electromechanical coupling is between the mean and relative shear strains of the core and the transverse electric field component. For the practical case of uniform potential, this is the only non-vanishing virtual work of Equation (20). Moreover, for an actuation problem ($\delta E_z = 0$),

the piezoelectric internal virtual work reduces to the shear one which can be written using Equations $(6)_2$ and $(8)_2$ as

$$\delta W^p_{\text{int}} = \delta W^p_{\gamma} = -\int_A \left[\frac{\delta\bar{u}}{R_s} + \frac{\partial\delta w}{\partial s} - \left(\frac{\bar{h}}{h_c} + \frac{\tilde{h}}{4R_s}\right)\bar{\beta}\right] e_{35}\tilde{\varphi} dA - \int_A \left[\frac{\delta\tilde{u}}{h_c} - \frac{1}{4}\left(\frac{\tilde{h}}{h_c} + \frac{\bar{h}}{R_s}\right)\tilde{\beta}\right] e_{35}\tilde{\varphi} dA \quad (24)$$

This expression was first presented in (Benjeddou, 2000c). It indicates that the shear piezoelectric action depends on the piezoelectric shear constant e_{35}, applied voltage difference $\tilde{\varphi}$, face to core thickness ratios $\bar{h}/h_c$, $\tilde{h}/h_c$ and shell shallowness $\bar{h}/R_s$, $\tilde{h}/R_s$. It proves also the importance of the transverse shear resulting from the sliding of the elastic faces against the piezoelectric core, represented by the first term of the second integral in Equation (24). The latter also shows the usefulness of retaining the mean and relative displacements as model independent variables. The presence of the shell meridian curvature $1/R_s$ couples membrane and bending behaviors. Hence, the pin-force model should be handled with great care if retained to represent the piezoelectric effect (Lalande et al., 1995).

ELECTRIC INTERNAL VIRTUAL WORK

Substituting the electric field Equation (8) into that of the electric virtual work (14), gives

$$\delta W^e_{\text{int}} = \int_A \left(\langle\delta\bar{E}\rangle\left[\bar{\epsilon}_p\right]\left\{\bar{E}\right\} + \langle\delta\tilde{E}\rangle\left[\tilde{\epsilon}_p\right]^T\left\{\tilde{E}\right\}\right) dA + \int_A \delta E_z \bar{\epsilon}_{zz} E_z dA \quad (25)$$

with

$$[\bar{\epsilon}_p] = h_c[\epsilon_p], \quad [\tilde{\epsilon}_p] = \frac{h_c^3}{12}[\epsilon_p], \quad \bar{\epsilon}_{zz} = h_c\,\epsilon_{zz}$$

The dielectric matrix $[\epsilon_p]$ is given in Appendix A. For uniform potentials, the electric virtual work (25) reduces to its last integral.

Sandwich Shell Inertia Virtual Work

The inertia virtual work of the sandwich shell can be defined as

$$\delta W_{in} = -\sum_{k=a}^{c}\int_{\Omega^k} \langle\delta\underline{u}^k\rangle\rho^k\left\{\delta\ddot{\underline{u}}^k\right\} d\Omega^k \quad (26)$$

where ρ^k, $k = a, b, c$, are the layers mass densities, and '..' states for time second derivative.

Substituting the displacements (3,4) in the previous equation, integrating through the shell thickness and decomposing into translation, (u), translation–rotary, ($u\beta$), and rotary, (β), contributions lead to the following expression for the inertia virtual work

$$\delta W_{in} = \delta W_u + \delta W_{u\beta} + \delta W_{\beta} \quad (27)$$

where the translation inertia virtual work δW_u has the form

$$\delta W_u = \int_A \left(\langle\delta\bar{d}_t\rangle\bar{\rho}_u\left\{\ddot{\bar{d}}_t\right\} + \langle\delta\bar{d}_p\rangle\tilde{\bar{\rho}}_u\left\{\ddot{\tilde{d}}_p\right\}\right) dA + \int_A \left(\langle\delta\tilde{d}_p\rangle\tilde{\bar{\rho}}_u\left\{\ddot{\bar{d}}_p\right\} + \langle\delta\tilde{d}_p\rangle\tilde{\rho}_u\left\{\ddot{\tilde{d}}_p\right\}\right) dA \quad (28)$$

with

$$\langle\bar{d}_t\rangle = \langle\,\bar{u} \quad \bar{v} \quad w\,\rangle, \quad \langle\bar{d}_p\rangle = \langle\,\bar{u} \quad \bar{v}\,\rangle, \quad \langle\tilde{d}_p\rangle = \langle\,\tilde{u} \quad \tilde{v}\,\rangle$$

The translation mass densities are given in Appendix C. They show that the mean-relative in-plane displacement inertia coupling vanishes for symmetric sandwich shells.

The translation–rotary inertia virtual work can be written as

$$\delta W_{u\beta} = \int_A \left(\langle\delta\bar{d}_p\rangle\bar{\rho}_{u\beta}\left\{\ddot{\bar{d}}_r\right\} + \langle\delta\bar{d}_r\rangle\bar{\rho}_{u\beta}\left\{\ddot{\bar{d}}_p\right\}\right) dA + \int_A \left(\langle\delta\bar{d}_p\rangle\tilde{\bar{\rho}}_{u\beta}\left\{\ddot{\tilde{d}}_r\right\} + \langle\delta\tilde{d}_r\rangle\tilde{\bar{\rho}}_{u\beta}\left\{\ddot{\bar{d}}_p\right\}\right) dA + \int_A \left(\langle\delta\tilde{d}_p\rangle\tilde{\bar{\rho}}_{\beta u}\left\{\ddot{\bar{d}}_r\right\} + \langle\delta\bar{d}_r\rangle\tilde{\bar{\rho}}_{\beta u}\left\{\ddot{\tilde{d}}_p\right\}\right) dA + \int_A \left(\langle\delta\tilde{d}_p\rangle\tilde{\rho}_{u\beta}\left\{\ddot{\bar{d}}_r\right\} + \langle\delta\tilde{d}_r\rangle\tilde{\rho}_{u\beta}\left\{\ddot{\tilde{d}}_p\right\}\right) dA \quad (29)$$

with

$$\langle\bar{d}_r\rangle = \langle\,\bar{\beta} \quad \bar{\beta}_\theta\,\rangle, \quad \langle\tilde{d}_r\rangle = \langle\,\tilde{\beta} \quad \tilde{\beta}_\theta\,\rangle$$

The translation–rotary mass densities, given in the Appendix C, indicate that there are four types of inertial couplings confined to the core layer

- A geometrical coupling between the *mean in-plane displacements* and *rotations* which vanishes for equal thickness faces.
- A coupling between the *mean in-plane displacements* and *relative rotations*.
- A coupling between the *relative in-plane displacements* and *mean rotations*.
- A geometrical coupling between the *relative in-plane displacements* and *rotations*, which vanishes for equal thickness faces.

The rotary inertia virtual work has the following expression

$$\delta W_\beta = \int_A \left(\langle \delta \bar{d}_r \rangle \bar{\rho}_\beta \left\{ \ddot{\bar{d}}_r \right\} + \langle \delta \bar{d}_r \rangle \tilde{\bar{\rho}}_\beta \left\{ \ddot{\tilde{d}}_r \right\} \right) dA + \int_A \left(\langle \delta \tilde{d}_r \rangle \tilde{\bar{\rho}}_\beta \left\{ \ddot{\bar{d}}_r \right\} + \langle \delta \tilde{d}_r \rangle \tilde{\rho}_\beta \left\{ \ddot{\tilde{d}}_r \right\} \right) dA \quad (30)$$

where the rotary mass densities are also given in Appendix C. Again, an inertial coupling between the mean and relative rotations appears in Equation (30) which vanishes for symmetric sandwich constructions.

Sandwich Shell External Virtual Work

The adaptive sandwich shell is supposed to support mechanical body, $f_{bs}^k, f_{b\theta}^k, f_{bz}^k$ and surface, F_s^k, F_θ^k, F_z^k, forces but free of electric body and surface charge densities. Hence, the external virtual work can be written as

$$\delta W_{ext} = \sum_{k=a}^{c} \left(\int_{\Omega^k} \langle \delta \underline{u}^k \rangle \left\{ f_b^k \right\} d\Omega^k + \int_{S_f^k} \langle \delta \underline{u}^k \rangle \left\{ F^k \right\} dS_f^k \right) \quad (31)$$

with $\langle f_b^k \rangle = \langle f_{bs}^k \ f_{b\theta}^k \ f_{bz}^k \rangle$, $\langle F^k \rangle = \langle F_s^k \ F_\theta^k \ F_z^k \rangle$. S_f^k is the kth layer boundary part where the surface forces $\langle \mathrm{F^k} \rangle$ are applied.

Substituting the displacement fields (3,4) into Equation (31) and integrating through the shell thickness, the external virtual work can be decomposed into

$$\delta W_{\text{ext}} = \delta W_{\text{ext}}^d + \delta W_{\text{ext}}^C \quad (32)$$

where δW_{ext}^d, δW_{ext}^C are the virtual works of external distributed (or surface) and concentrated (or line) loads. These are defined in the following sub-sections.

EXTERNAL VIRTUAL WORK OF DISTRIBUTED LOADS

From the body forces, the following surface loads are introduced for the kth layer

$$\left\{ f^k \right\} = \int_z \left\{ f_b^k \right\} dz, \quad \left\{ m^k \right\} = \int_z \left\{ f_b^k \right\} (z - z_k) dz \quad (33)$$

With these definitions in mind, the external virtual work due to body forces is

$$\delta W_{\text{ext}}^d = \int_A \left(\langle \delta \bar{d}_t \rangle \left\{ \bar{f} \right\} + \langle \delta \bar{d}_r \rangle \{ \bar{m} \} \right) dA + \int_A \left(\langle \delta \tilde{d}_p \rangle \left\{ \tilde{f} \right\} + \langle \delta \tilde{d}_r \rangle \{ \tilde{m} \} \right) dA \quad (34)$$

where the mean and relative forces and moments per unit area are given in Appendix D. They are of course applied on the shell mid-surface. However, if the shell is subjected to distributed forces F_s^+, F_θ^+, F_z^+ and F_s^-, F_θ^-, F_z^- on the inner and outer surfaces, respectively, above expression (34) can be still used but with different expressions of the mean and relative distributed loads. In this case, Equation (34) becomes

$$\delta W_{\text{ext}}^d = \int_A \left(\langle \delta \bar{d}_t \rangle \left\{ \bar{f}_d \right\} + \langle \delta \bar{d}_r \rangle \{ \bar{m}_d \} \right) dA + \int_A \left(\langle \delta \tilde{d}_p \rangle \left\{ \tilde{f}_d \right\} + \langle \delta \tilde{d}_r \rangle \{ \tilde{m}_d \} \right) dA \quad (35)$$

where the mean and relative distributed forces and moments are given in Appendix D.

EXTERNAL VIRTUAL WORK OF CONCENTRATED LOADS

Using definitions (33) to introduce the line loads (per unit length) from the surface ones $\{F^{Sk}\}$, the external virtual work δW_{ext}^C of these concentrated loads is

$$\delta W_{\text{ext}}^C = \int_{S_F} (\langle \delta \bar{d}_t \rangle \{ \bar{F} \} + \langle \delta \bar{d}_r \rangle \{ \bar{M} \}) ds_c + \int_{S_F} \left(\langle \delta \tilde{d}_p \rangle \{ \tilde{F} \} + \langle \delta \tilde{d}_r \rangle \{ \tilde{M} \} \right) ds_c \quad (36)$$

where $ds_c = \pm\, ds$ for distributed loads along the meridian and $ds_c = \pm\, r d\theta$ for distributed loads along the circumference. ds_c represents the curvilinear abscissa of a curve on the mid-surface A of the sandwich shell. For example, for a closed shell of revolution, expression (36) can be simplified to

$$\delta W_{\text{ext}}^C = \int_\theta \left[(\langle \delta \bar{d}_t \rangle \{ \bar{F} \} + \langle \delta \bar{d}_r \rangle \{ \bar{M} \}) r \right]_{s_f} d\theta + \int_\theta \left[(\langle \delta \tilde{d}_p \rangle \{ \tilde{F} \} + \langle \delta \tilde{d}_r \rangle \{ \tilde{M} \}) r \right]_{s_f} d\theta \quad (37)$$

where s_f is here the circumference at fixed curvilinear abscissa s. The mean and relative line force and moment vectors are given for this case in Appendix D.

CONCLUSION

A theoretical formulation has been presented for adaptive sandwich shells of revolution. It has the originality to use the transverse shear response of a piezoelectric core sandwiched between two elastic layers. The former has been assumed poled along its meridian and covered with electrodes on its inner and outer skins. Hence, for the practical case of uniform electric potentials, the electromechanical coupling is between the transverse shear strains and the transverse electric field. The formulation uses the mean and relative

displacements and rotations of the faces middle surfaces as independent mechanical variables. These are augmented by the mean and relative potentials of the piezoelectric core in order to consider effectively the electromechanical coupling. This choice of independent mechanical and electric variables has the advantage of representing explicitly the transverse shear electromechanical response of the piezoelectric core. It has also permitted to decompose all quantities of the formulation (strains, electric field, virtual works, etc.) into mean and relative contributions. This will facilitate the finite element implementation of the present formulation as will be shown in Part 2 of this paper.

APPENDIX

A. Piezoelectric Reduced Constitutive Equations

The three-dimensional constitutive equations of a piezoelectric material polarized along its first material axis can be written for its converse and direct effects, respectively, as

$$\begin{aligned} \{T\} &= [C]\{S\} - [e]^T\{E\} \\ \{D\} &= [e]\{S\} + [\in]\{E\} \end{aligned} \tag{A1}$$

with

$$\langle T\rangle = \langle T_1\ T_2\ T_3\ T_4\ T_5\ T_6\rangle, \quad \langle E\rangle = \langle E_1\ E_2\ E_3\rangle$$
$$\langle S\rangle = \langle S_1\ S_2\ S_3\ S_4\ S_5\ S_6\rangle, \quad \langle D\rangle = \langle D_1\ D_2\ D_3\rangle$$

$\{T\}, \{S\}, \{D\}, \{E\}$ are the vectors of stress, strain, electric displacement and field components. $[C]$, $[e]$ and $[\in]$ are the elastic, piezoelectric and dielectric matrices given by

$$[e] = \begin{bmatrix} e_{11} & e_{12} & e_{13} & 0 & 0 & 0 \\ 0 & 0 & 0 & 0 & 0 & e_{26} \\ 0 & 0 & 0 & 0 & e_{35} & 0 \end{bmatrix},$$
$$[\in] = \begin{bmatrix} \in_{11} & 0 & 0 \\ 0 & \in_{22} & 0 \\ 0 & 0 & \in_{33} \end{bmatrix}$$
$$[C] = \begin{bmatrix} C_{11} & C_{12} & C_{13} & 0 & 0 & 0 \\ C_{12} & C_{22} & C_{23} & 0 & 0 & 0 \\ C_{13} & C_{23} & C_{33} & 0 & 0 & 0 \\ 0 & 0 & 0 & C_{44} & 0 & 0 \\ 0 & 0 & 0 & 0 & C_{55} & 0 \\ 0 & 0 & 0 & 0 & 0 & C_{66} \end{bmatrix} \tag{A2}$$

It is worthwhile to notice that the piezoelectric material constants of these matrices can be obtained from those of the through-thickness polarized piezoelectric materials through matrix transformations. See (Benjeddou, 2000c) for the detailed corresponding derivation.

Applying the zero normal stress condition ($\sigma_3 = 0$), the converse constitutive Equations (A1) reduce to the following converse in-plane and transverse ones

$$\begin{aligned} \{\sigma\} &= [Q]\{\varepsilon\} - [e_p]^T\{E_p\} \\ \{\tau\} &= [Q_s]\{\gamma\} - \{e_s\}E_3 \end{aligned} \tag{A3}$$

with

$$\langle\sigma\rangle = \langle\sigma_1\ \sigma_2\ \sigma_6\rangle,\ \langle\tau\rangle = \langle\sigma_4\ \sigma_5\rangle, \langle E_p\rangle = \langle E_1\ E_2\rangle,$$
$$\langle\varepsilon\rangle = \langle\varepsilon_1\ \varepsilon_2\ \varepsilon_6\rangle, \quad \langle\gamma\rangle = \langle\varepsilon_4\ \varepsilon_5\rangle$$

The in-plane and transverse elastic and piezoelectric matrices are given by

$$[Q] = \begin{bmatrix} Q_{11} & Q_{12} & 0 \\ Q_{12} & Q_{22} & 0 \\ 0 & 0 & Q_{66} \end{bmatrix}, \quad [e_p] = \begin{bmatrix} \hat{e}_{11} & \hat{e}_{12} & 0 \\ 0 & 0 & e_{26} \end{bmatrix}$$
$$[Q_s] = \begin{bmatrix} Q_{44} & 0 \\ 0 & Q_{55} \end{bmatrix}, \quad \langle e_s\rangle = \langle\, 0 \quad e_{35}\,\rangle \tag{A4}$$

with

$$Q_{11} = C_{11} - C_{13}\frac{C_{13}}{C_{33}}, \quad Q_{22} = C_{22} - C_{23}\frac{C_{23}}{C_{33}}$$
$$Q_{12} = C_{12} - C_{23}\frac{C_{13}}{C_{33}}, \quad Q_{66} = C_{66}, \quad Q_{44} = C_{44}, \quad Q_{55} = C_{55}$$
$$\hat{e}_{11} = e_{11} - e_{13}\frac{C_{13}}{C_{33}}, \quad \hat{e}_{12} = e_{12} - e_{13}\frac{C_{23}}{C_{33}}$$

The direct in-plane and transverse piezoelectric constitutive equations can also be reduced from Equation (A1) using the zero normal stress assumption, as follows

$$\begin{aligned} \{D_p\} &= [e_p]\{\varepsilon\} + [\in_p]\{E_p\} \\ D_3 &= \langle e_s\rangle\{\gamma\} + \in_{33} E_3 \end{aligned} \tag{A5}$$

with

$$[\in_p] = \begin{bmatrix} \hat{\in}_{11} & 0 \\ 0 & \in_{22} \end{bmatrix}, \quad \hat{\in}_{11} = \in_{11} + e_{13}\frac{e_{13}}{C_{33}}$$

B. Composite Electromechanical Constant Matrices

The elastic mean, mean-relative and relative membrane matrices of the sandwich shell are

$$\begin{aligned} [\bar{D}_e] &= h_a[Q^a] + h_b[Q^b] + h_c[Q^c] \\ [\tilde{\bar{D}}_e] &= \frac{1}{2}(h_a[Q^a] - h_b[Q^b]) \\ [\tilde{D}_e] &= \frac{1}{4}(h_a[Q^a] + h_b[Q^b]) + \frac{h_c}{12}[Q^c] \end{aligned} \tag{B1}$$

The composite membrane-bending mean, mean-relative, relative-mean and relative elastic matrices are defined by

$$\begin{aligned}
&[\bar{D}_{e\chi}] = -\frac{\tilde{h}}{4} h_c [Q^c], \quad \left[\tilde{\bar{D}}_{e\chi}\right] = -\frac{\bar{h}}{4} h_c [Q^c] \\
&\left[\tilde{\bar{D}}_{\chi e}\right] = -\bar{h}\frac{h_c}{12}[Q^c], \quad \left[\tilde{\mathbf{D}}_{e\chi}\right] = -\frac{\tilde{h}}{4}\frac{h_c}{12}[Q^c]
\end{aligned} \tag{B2}$$

The composite bending mean, mean-relative and relative elastic matrices have the form

$$\begin{aligned}
[\bar{D}_\chi] &= \frac{h_a^3}{12}[Q^a] + \frac{h_b^3}{12}[Q^b] + \left(\frac{\tilde{h}^2}{16} + \frac{\bar{h}^2}{12}\right) h_c [Q^c] \\
\left[\tilde{\bar{D}}_\chi\right] &= \frac{1}{2}\left(\frac{h_a^3}{12}[Q^a] - \frac{h_b^3}{12}[Q^b]\right) + \frac{\tilde{h}}{4}\frac{\bar{h}}{3} h_c [Q^c] \\
[\tilde{D}_\chi] &= \frac{1}{4}\left(\frac{h_a^3}{12}[Q^a] + \frac{h_b^3}{12}[Q^b]\right) + \left(\frac{\tilde{h}^2}{192} + \frac{\bar{h}^2}{16}\right) h_c [Q^c]
\end{aligned} \tag{B3}$$

The faces and core, mean, mean-relative and relative shear elastic matrices are

$$\begin{aligned}
&[\bar{D}_\gamma] = h_a [Q_s^a] + h_b [Q_s^b], \quad [\tilde{\bar{D}}_\gamma] = \tfrac{1}{2}\left(h_a [Q_s^a] - h_b [Q_s^b]\right) \\
&[\tilde{D}_\gamma] = \tfrac{1}{4}\left(h_a [Q_s^a] + h_b [Q_s^b]\right), \quad [\tilde{D}_\gamma^c] = [\tilde{\bar{D}}_\gamma^c] = [\tilde{D}_\gamma^c] = h_c [Q_s^c]
\end{aligned} \tag{B4}$$

The extension, bending and shear mean and relative composite piezoelectric matrices have the following expressions, respectively

$$\begin{aligned}
&[\bar{D}_e^p] = h_c [e_p], \quad [\tilde{D}_e^p] = \frac{h_c^2}{12}[e_p] \\
&[\bar{D}_\chi^p] = -\frac{\tilde{h}}{4} h_c [e_p], \quad \left[\tilde{\bar{D}}_\chi^p\right] = -\bar{h}\frac{h_c^2}{12}[e_p] \\
&\left[\tilde{\bar{D}}_\chi^p\right] = -\frac{\bar{h}}{4} h_c [e_p], \quad [\tilde{D}_\chi^p] = -\frac{\tilde{h}}{4}\frac{h_c^2}{12}[e_p] \\
&\left\{\bar{D}_\gamma^p\right\} = \left\{\tilde{D}_\gamma^p\right\} = h_c \{e_s\}
\end{aligned} \tag{B5}$$

C. Composite Mass Densities

The composite mean, mean-relative and relative mass densities of the sandwich shell are

$$\begin{aligned}
\bar{\rho}_u &= h_a \rho^a + h_b \rho^b + h_c \rho^c \\
\tilde{\bar{\rho}}_u &= \frac{1}{2}(h_a \rho^a - h_b \rho^b) \\
\tilde{\rho}_u &= \frac{1}{4}(h_a \rho^a + h_b \rho^b) + \frac{h_c}{12}\rho^c
\end{aligned} \tag{C1}$$

The translation-rotary mean, mean-relative, relative-mean and relative mass densities of the composite shell have the following form

$$\begin{aligned}
&\bar{\rho}_{u\beta} = -\frac{\tilde{h}}{4} h_c \rho^c, \quad \tilde{\bar{D}}_{u\beta} = -\frac{\bar{h}}{4} h_c \rho^c \\
&\tilde{\bar{\rho}}_{\beta u} = -\bar{h}\frac{h_c}{12}\rho^c, \quad \tilde{\rho}_{u\beta} = -\frac{\tilde{h}}{4}\frac{h_c}{12}\rho^c
\end{aligned} \tag{C2}$$

The rotary mean, mean-relative and relative mass densities of the composite shell are

$$\begin{aligned}
\bar{\rho}_\beta &= \frac{h_a^3}{12}\rho^a + \frac{h_b^3}{12}\rho^b + \left(\frac{\tilde{h}^2}{16} + \frac{\bar{h}^2}{12}\right) h_c \rho^c \\
\tilde{\bar{\rho}}_\beta &= \frac{1}{2}\left(\frac{h_a^3}{12}\rho^a - \frac{h_b^3}{12}\rho^b\right) + \frac{\tilde{h}}{4}\frac{\bar{h}}{3} h_c \rho^c \\
\tilde{\rho}_\beta &= \frac{1}{4}\left(\frac{h_a^3}{12}\rho^a + \frac{h_b^3}{12}\rho^b\right) + \left(\frac{\tilde{h}^2}{192} + \frac{\bar{h}^2}{16}\right) h_c \rho^c
\end{aligned} \tag{C3}$$

Notice the full analogy between the composite matrices (B1–B3) of the mechanical constants and the present mass density relations (C1–C3).

D. Composite Surface and Line External Loads

The mean and relative surface forces (per unit area) that can be applied to the composite shell are

$$\begin{aligned}
\bar{f}_s &= f_s^a + f_s^b + f_s^c \quad \tilde{f}_s = \frac{1}{2}(f_s^a - f_s^b) + \frac{m_s^c}{h_c} \\
\bar{f}_\theta &= f_\theta^a + f_\theta^b + f_\theta^c, \\
\bar{f}_z &= f_z^a + f_z^b + f_z^c \quad \tilde{f}_\theta = \frac{1}{2}(f_\theta^a - f_\theta^b) + \frac{m_s^c}{h_c}
\end{aligned} \tag{D1}$$

where, for $k = a, b, c$

$$\begin{Bmatrix} f_s^k \\ f_\theta^k \\ f_z^k \end{Bmatrix} = \int_z \begin{Bmatrix} f_{bs}^k \\ f_{b\theta}^k \\ f_{bz}^k \end{Bmatrix} dz, \quad \begin{Bmatrix} m_s^k \\ m_\theta^k \end{Bmatrix} = \int_z \begin{Bmatrix} f_{bs}^k \\ f_{b\theta}^k \end{Bmatrix} (z - z_k) dz$$

$f_{sb}^k, f_{\theta b}^k, f_{zb}^k$ are the body forces (per unit volume) that the shell is supposed to support.

The mean and relative surface moments (per unit area) that the sandwich shell can support are defined by the following expressions

$$\begin{aligned}
\bar{m}_s &= m_s^a + m_s^b - \frac{\bar{h}}{h_c} m_s^c - \frac{\tilde{h}}{4} f_s^c \\
\bar{m}_\theta &= m_\theta^a + m_\theta^b - \frac{\bar{h}}{h_c} m_\theta^c - \frac{\tilde{h}}{4} f_\theta^c \\
\tilde{m}_s &= \frac{1}{2}(m_s^a - m_s^b) - \frac{\tilde{h}}{4h_c} m_s^c - \frac{\bar{h}}{4} f_s^c \\
\tilde{m}_\theta &= \frac{1}{2}(m_\theta^a - m_\theta^b) - \frac{\tilde{h}}{4h_c} m_\theta^c - \frac{\bar{h}}{4} f_\theta^c
\end{aligned} \tag{D2}$$

The mean and relative distributed forces due to applied surface forces F_s^+, F_θ^+, F_z^+ and F_s^-, F_θ^-, F_z^- to the inner and outer sandwich shell skins, respectively, are

$$\begin{aligned} \bar{f}_s^d &= F_s^+ + F_s^- \quad \tilde{f}_s^d = \tfrac{1}{2}(F_s^+ - F_s^-) \\ \bar{f}_\theta^d &= F_\theta^+ + F_\theta^-, \\ \bar{f}_z^d &= F_z^+ + F_z^- \quad \tilde{f}_\theta^d = \tfrac{1}{2}(F_\theta^+ - F_\theta^-) \end{aligned} \tag{D3}$$

The following relations give the corresponding mean relative distributed moments

$$\begin{aligned} \bar{m}_s^d &= \tfrac{1}{2}(h_a F_s^+ - h_b F_s^-) \quad \tilde{m}_s^d = \tfrac{1}{4}(h_a F_s^+ + h_b F_s^-) \\ \bar{m}_\theta^d &= \tfrac{1}{2}(h_a F_\theta^+ - h_b F_\theta^-) \quad \tilde{m}_\theta^d = \tfrac{1}{4}(h_a F_\theta^+ + h_b F_\theta^-) \end{aligned} \tag{D4}$$

It is worthwhile to notice that relations (D3) and (D4) can be obtained from the corresponding ones (D1) and (D2), as a particular case. In fact, since the core is not loaded in this case, its corresponding terms in (D1) and (D2) should be omitted and to obtain equations (D3) and (D4) the following relations have to be considered

$$\begin{aligned} f_s^a &= F_s^+, \quad f_\theta^a = F_\theta^+, \quad f_z^a = F_z^+ \\ f_s^b &= F_s^-, \quad f_\theta^b = F_\theta^-, \quad f_z^b = F_z^- \\ m_s^a &= \frac{h_a}{2} F_s^+, \quad m_\theta^a = \frac{h_a}{2} F_\theta^+ \\ m_s^b &= -\frac{h_b}{2} F_s^-, \quad m_\theta^b = -\frac{h_b}{2} F_\theta^- \end{aligned} \tag{D5}$$

The mean and relative line forces (per unit length) that can be applied to the sandwich shell are

$$\begin{aligned} \bar{F}_s &= F_s^a + F_s^b + F_s^c \quad \tilde{F}_s = \frac{1}{2}(F_s^a - F_s^b) + \frac{M_s^c}{h_c} \\ \bar{F}_\theta &= F_\theta^a + F_\theta^b + F_\theta^c, \\ \bar{F}_z &= F_z^a + F_z^b + F_z^c \quad \tilde{F}_\theta = \frac{1}{2}(F_\theta^a - F_\theta^b) + \frac{M_\theta^c}{h_c} \end{aligned} \tag{D6}$$

where, for $k = a, b, c$

$$\begin{Bmatrix} F_s^k \\ F_\theta^k \\ F_z^k \end{Bmatrix} = \int_z \begin{Bmatrix} F_s^{Sk} \\ F_\theta^{Sk} \\ F_z^{Sk} \end{Bmatrix} dz, \quad \begin{Bmatrix} M_s^k \\ M_\theta^k \end{Bmatrix} = \int_z \begin{Bmatrix} F_s^{Sk} \\ F_\theta^{Sk} \end{Bmatrix} (z - z_k) dz$$

F_s^{Sk}, F_θ^{Sk}, F_z^{Sk} are the surface forces (per unit area) applied to a circumference or meridian cross section of the kth layer of the sandwich shell of revolution.

The corresponding mean and relative line moments are given by

$$\bar{M}_s = M_s^a + M_s^b - \frac{\bar{h}}{h_c} M_s^c - \frac{\tilde{h}}{4} F_s^c$$

$$\bar{M}_\theta = M_\theta^a + M_\theta^b - \frac{\bar{h}}{h_c} M_\theta^c - \frac{\tilde{h}}{4} F_\theta^c$$

$$\tilde{M}_s = \frac{1}{2}(M_s^a - M_s^b) - \frac{\tilde{h}}{4h_c} M_s^c - \frac{\bar{h}}{4} F_s^c$$

$$\tilde{M}_\theta = \frac{1}{2}(M_\theta^a - M_\theta^b) - \frac{\tilde{h}}{4h_c} M_\theta^c - \frac{\bar{h}}{4} F_\theta^c$$

Notice the complete analogy between the expressions of the surface loads (D1) and (D2) and the corresponding line loads given by (D6) and (D7), respectively.

REFERENCES

Adelman, N.T. and Stavsky, Y. (1975). Radial vibrations of axially polarized piezoelectric ceramic cylinders. *J. Acoust. Soc. Am.*, **57**: 356–360.

Aldraihem, O.J. and Khdeir, A. (2000). Smart beams with extension and thickness shear piezoelectric actuators. *Smart Mater., Struct.*, **9**: 1–9.

Aoyagi, M., Murasawa, Y., Ocasawara, T. and Tomikawa, Y. (1977). Experimental characteristics of a bolt-clamped short-cylindrical torsional vibrator using shear mode piezoceramics inserted in the axial direction. *Jpn. J. Appl. Phys.*, **36**: 3126–3129.

Benjeddou, A. (2000a). Advances in piezoelectric finite element modeling of adaptive structural elements: a survey. *Comput. Struct.*, **76**: 347–363.

Benjeddou, A. (2000b). Transverse shear piezoelectric actuation of shells. In: Papadrakakis, M., Samartin, A. and Oñate, E. (Eds.), *4th Int. Colloq. on Computation of Shell and Spatial Structures*, Athens (Greece): ISASR–NTUA.

Benjeddou, A. (2000c). Piezoelectric transverse shear actuation of shells of revolution: theoretical formulation and analysis. *Europ. Congr. on Computational Methods in Appl. Sc. and Engng.* (*ECCOMAS*), Barcelona (Spain), (Invited Lecture).

Benjeddou, A. and Hamdi, M.A. (1996). A B-spline finite element for the dynamic analysis of sandwich shells of revolution. *Engrg. Computations*, **13**: 241–264.

Benjeddou, A., Trindade, M.A. and Ohayon, R. (1997). A unified beam finite element model for extension and shear piezoelectric actuation mechanisms. *J. Intell. Mater. Syst. Struct.*, **8**: 1012–1025.

Benjeddou, A., Trindade, M.A. and Ohayon, R. (1999a). A new shear actuated smart structure beam finite element. *AIAA J.*, **37**: 378–383.

Benjeddou, A., Trindade, M.A. and Ohayon, R. (1999b). Two models for two actuation mechanisms: a comparison. In: Weber, H.I., Goncalves, P.B., Jasiuk, I., Pamplona, D. Steele, C. and Bevilaqua, L. *Applied Mechanics in the Americas*. **8**: 1545–1548.

Benjeddou, A., Trindade, M.A., Ohayon, R. (2000). Piezoelectric actuation mechanisms for intelligent sandwich structures. *Smart Mater. Struct.*, **9**: 328–335.

Boriseiko, V.A., Martynenko, V.S. and Ulitko, A.F. (1979). Relations of electroelasticity of piezoceramic shells of revolution polarized along the meridional co-ordinate. *Prikladnaia Mekhanica*, **15**: 1155

Bradley, Jr. W. and Bergman, G.B. (1963). US Patent 3,104,334.

Centalanza, L.R. and Smith, E.C. (2000). Design and experimental testing of an induced shear piezoelectric actuator for rotor blade trailing edge flags. AIAA paper # 2000–1713.

Glazounov, A.E., Wang S., Zhang, Q.M. and Kim, C. (1999). High-efficiency piezoelectric motor combining continuous rotation with precise control over angular positioning. *Appl. Phys. Lett.*, **75**: 862–864.

Glazounov, A.E., Wang, S., Zhang, Q.M. and Kim, C. (2000). Piezoelectric stepper motor with direct coupling mechanism to achieve high efficiency and precise control of motion. *IEEE Trans. on Ultrasonics, Ferroelectrics, and Freq. Control,* **47**: 1059–1067.

Glazounov, A.E., Zhang, Q.M. and Kim, C. (1998). Piezoelectric actuator generating torsional displacement from piezoelectric d_{15} shear response. *Appl. Phys. Lett*., **72**: 2526–2528.

Glazounov, A.E., Zhang, Q.M. and Kim, C. (2000). Torsional actuator based on mechanically amplified shear piezoelectric response. *Sensors and Actuators: A Physical*, **79**: 22–30.

Lalande, F., Chaudhry, Z. and Rogers, C.A. (1995). Modeling considerations for in-phase actuation of actuators bonded to shell structures. *AIAA J*., **33**: 1300–1305.

Parton, V.Z. and Senik, N.A. (1984). On the application of the method of symbolic integration in the theory of piezoceramic shells. *PMM USSR*, **47**: 214–219.

Rogacheva, N.N. (1981). Equations of state of piezoceramic shells *PMM USSR*, **45**: 677–684.

Saravanos, A. and Heyliger, P.R. (1999). Mechanics and computational models for laminated piezoelectric beams, plates and shells. *Appl. Mech. Rev*., **52**:305–320.

Sun, C.T. and Zhang, X.D. (1995). Use of thickness-shear mode in adaptive sandwich structures. *Smart Mater. Struct*., **4**: 202–206.

Trindade, M.A., Benjeddou, A., Ohayon, R. (1999). Parametric analysis of the vibration control of sandwich beams through shear-based piezoelectric actuation. *J. Intell. Mater. Syst. Struct*., **10**: 377–385.

Zhang, X.D. and Sun, C.T. (1996) Formulation of an adaptive sandwich beam. *Smart Mater. Struct*., **5**: 814–823.

Zhang, X.D. and Sun, C.T. (1999). Analysis of a sandwich plate containing a piezoelectric core. *Smart Mater*., *Struct*., **8**: 31–40.